



## Adsorption characterizations of biosorbent extracted from waste activated sludge for Pb(II) and Zn(II)

Yun Zhou<sup>a,b</sup>, Siqing Xia<sup>b</sup>, Jiao Zhang<sup>c</sup>, Zhiqiang Zhang<sup>a,b,d,\*</sup>,  
Slawomir W. Hermanowicz<sup>d,e</sup>

<sup>a</sup>Key Laboratory of Yangtze River Water Environment, Ministry of Education, College of Environmental Science and Engineering, Tongji University, Shanghai 200092, China, Tel. +86 21 65984268; email: [zhouyun06@126.com](mailto:zhouyun06@126.com) (Y. Zhou), Tel. +86 21 65981831; email: [zhiqiang@tongji.edu.cn](mailto:zhiqiang@tongji.edu.cn) (Z. Zhang)

<sup>b</sup>State Key Laboratory of Pollution Control and Resource Reuse, College of Environmental Science and Engineering, Tongji University, Shanghai 200092, China, Tel. +86 21 65980440; email: [siqingxia@tongji.edu.cn](mailto:siqingxia@tongji.edu.cn) (S. Xia)

<sup>c</sup>School of Civil Engineering and Transportation, Shanghai Technical College of Urban Management, Shanghai 200432, China, Tel. +86 21 65743348; email: [gglg@163.com](mailto:gglg@163.com) (J. Zhang)

<sup>d</sup>Department of Civil and Environmental Engineering, University of California, Berkeley, CA 94720, USA, Tel. +1 510 931 5453; email: [hermanowicz@ce.berkeley.edu](mailto:hermanowicz@ce.berkeley.edu) (S.W. Hermanowicz)

<sup>e</sup>National High-end Foreign Expert Program, Tongji University, Shanghai 200092, China

Received 12 July 2014; Accepted 8 March 2015

---

### ABSTRACT

The adsorption characterizations of the biosorbent extracted from waste activated sludge after short-time aerobic digestion were investigated by adsorbing Pb<sup>2+</sup> and Zn<sup>2+</sup> from aqueous single metal solutions. The adsorption kinetics were well fit for the pseudo-second-order model. Compared with Freundlich and Temkin models, Langmuir model better described the adsorption isotherms. The maximum adsorption capacities of the biosorbent (793.61 mg Pb<sup>2+</sup>/g and 408.38 mg Zn<sup>2+</sup>/g) were markedly higher than those of the reported biosorbents. Thermodynamic analyses indicated that the sorption processes were feasible and spontaneous in nature. The surface morphology of the biosorbent showed a meshy structure with small branches, which was ideal for the biosorbent to quickly capture the metal ions. The energy dispersive X-ray spectra confirmed that the adsorbed metal ions lay in the precipitates of the adsorption reactions. Fourier transform infrared analyses showed that the major functional groups are responsible for the adsorption. The adsorption of the biosorbent for Pb<sup>2+</sup> and Zn<sup>2+</sup> was mainly physisorption in nature enhanced by chemisorption. Complexation and ion exchange between the functional groups and the metal ions played an important role in the chemisorption.

*Keywords:* Heavy metal; Lead; Zinc; Biosorbent; Waste activated sludge; Adsorption mechanism

---

\*Corresponding author.

## 1. Introduction

Since heavy metals are used in various industries due to their technological importance, wastewater from these industries contains metal ions having a permanent toxic effect [1–3]. Lead ( $\text{Pb}^{2+}$ ) and zinc ( $\text{Zn}^{2+}$ ) are common metal ions found in many industrial wastewaters. All lead compounds are cumulative poisons that normally affect the gastrointestinal tract, the nervous system, and sometimes both [4]. What is more, millions of adults and children suffered adverse health effects and impaired intellectual development [5]. Among the Water Framework Directive, lead is one of the 11 hazardous priority substances in the list of pollutants which can be regarded as a long-lasting environmental pollutant. Zinc was reported to influence cell apoptosis by acting on several molecular regulators of programmed cell death, including caspases and proteins from the Bcl and Bax families [6]. According to the United States environmental protection agency, zinc is one of the 13 metals in the list of Priority Pollutants [7].

Various technologies have been reported for the treatment of water contaminated by trace toxic metals. The techniques usually involve the application of physicochemical processes such as precipitation, oxidation, reduction, adsorption, filtration, flocculation, sedimentation, osmosis, ion exchange, biosorption, etc. [7,8]. Among the techniques available, biosorption plays a significant role in the removal of heavy metals due to biodegradability, nontoxicity, and efficacy of biosorbents. Biosorption has been considered as a promising technology for the removal of heavy metals and uptake of contaminants by biological materials via various physicochemical mechanisms including ion exchange, complexation, microprecipitation, sorption, etc. [9–11].

Recently, extracellular polymeric substances (EPSs) have been described as trap for dissolved species [12,13] and has been noted for their tendency to avidly bind metals and dye [14,15]. They are micro-organism-produced macromolecules, majorly consisting of polysaccharides, proteins, and nucleic acids, begin to receive attention as novel biosorbents [16,17]. The removal of heavy metals by EPSs is attributed to a large number of negatively charged functional groups such as carboxyl, hydroxyl, amino, phosphate, and sulfate [17,18]. EPSs may contain nonpolymeric substituents of low molecular weight which greatly alter their structure and physicochemical properties. Thus, extracellular polysaccharides often carry organic substituents such as acetyl, succinyl, or pyruvyl groups or inorganic substituents such as sulfate. Proteins can be glycosylated with oligosaccharides to form glycoproteins or can be

substituted with fatty acids to form lipoproteins [17]. The matrix of correlation between the composition of the EPSs and the complexation parameters showed that the number of binding sites and the complexation constant were strongly linked to the contents of proteins, polysaccharides, and humic substances [19]. However, further application of these methods has not been reported because EPSs from micro-organisms or anaerobic sludge as biosorbent showed low productivity and weak adsorbability.

Containing a significant amount of natural organic macromolecule substances, the waste activated sludge (WAS) from municipal wastewater treatment plant (WWTP) is believed as a good source of EPSs [20]. During the early stage of aerobic digestion of WAS, the biochemical reactions are similar to those in the aerobic bioreactors for wastewater treatment, while the biodegradation of the newly produced macromolecules has not started. The EPS harvest from WAS at the early stage of aerobic digestion is meaningful to both EPS source and WAS stabilization. If the EPS was applied to the adsorption of heavy metals, it would not only help to make clear the adsorption characteristics of the EPS, but also help to understand the biological treatment of heavy metal-containing wastewater. Therefore, it appears interesting to investigate  $\text{Pb}^{2+}$  and  $\text{Zn}^{2+}$  adsorption by the EPS from WAS after short-time aerobic digestion.

In this study, the EPS from WAS after short-time aerobic digestion was used as a novel biosorbent for the removal of  $\text{Pb}^{2+}$  and  $\text{Zn}^{2+}$  from aqueous single metal solutions. The aims were to ascertain the adsorption characterizations of the biosorbent via kinetics, isotherm, and thermodynamic analyses, and further to explore the adsorption mechanisms of the toxic metals onto the biosorbent.

## 2. Materials and methods

### 2.1. Chemicals

A stock solution of lead and zinc was prepared by dissolving AR grade of  $\text{Pb}(\text{NO}_3)_2$  and  $\text{Zn}(\text{NO}_3)_2 \cdot 6\text{H}_2\text{O}$  in distilled water, respectively, at an initial concentration of 1,000 mg/L. pH was adjusted by HCl (0.1 mol/L) and  $\text{NH}_3 \cdot \text{H}_2\text{O}$  (0.1 mol/L).

### 2.2. WAS aerobic digestion

The WAS samples used for biosorbent extraction were obtained from the secondary settling tank back-flow sludge from a full-scale municipal WWTP in Shanghai, China. Anaerobic–anoxic–aerobic process

was used in the domestic WWTP with the capacity of 60,000 m<sup>3</sup>/d. After gravity concentration of the sludge, its main parameters were as following: pH 6.8–7.5, suspended solids (SS) 9.0 ± 1 g/L, and the ratio of volatile suspended solids to suspended solids (VSS/SS) 65 ± 8%. The aerobic digestion process of WAS was carried out under room temperature (about 20°C), natural sludge pH (about 7.0), and dissolved oxygen (DO) 2–3 mg/L. After the WAS was aerobically digested for about 4 h, it was ready for biosorbent extraction, which was according to the former experimental results of the parameter optimization.

### 2.3. Biosorbent preparation

Extraction of biosorbent was carried out with ultrasound followed by centrifugation. The ultrasound reactor was equipped with a transducer (20 kHz, diameter of 13 mm) according to the former study [21]. During ultrasonic treatment (power density 2.7 kW/L, pulse 4 s), the tip of the transducer was immersed at about 10-mm deep into 100-mL sludge samples to be processed for 2 min, and the temperature was maintained at about 298.15 [22]. Then, the treated sludge samples were centrifuged twice at 10,800 × g and 277.15 K for 10 min every time. The supernatant was the raw biosorbent.

To purify the EPS, three volumes of cold acetone were added into the crude liquid EPS. After staying in fridge (277.15 K) for about 12 h, the mixture was centrifuged at 277.15 K and 15,777 × g for 10 min. The obtained precipitate was redissolved in distilled water to the original volume, and then the above operations were repeated two times more. The precipitate obtained at the third time was dialyzed in distilled water overnight at 277.15 K, and finally was lyophilized to obtain the purified EPS [23]. Results showed that the biosorbent productivity of the WAS after 4-h aerobic digestion was 52.46-mg biosorbent/g VSS, increasing about 25.1% over that of the original WAS. Chemical analysis of the biosorbent indicated that it consisted of protein (50.5%, w/w), polysaccharide (30.1%, w/w), and nucleic acid (19.4%, w/w). The molecular weight of the biosorbent is about 2.97 × 10<sup>6</sup> Da, meaning that it is a natural organic macromolecule substance.

### 2.4. Kinetic studies

Throughout the adsorption kinetic experiments, reaction conditions were controlled as follows: reaction temperature 308.15 K, initial pH 6.0, initial concentrations of metal ions (Pb<sup>2+</sup> or Zn<sup>2+</sup>) 5, 20, and

50 mg/L, solution volume 50 mL, the weight ratio of biosorbent to metal ions 2.5/1. After adsorption, the solutions were separated from the precipitates by centrifugation at 10,800 × g for 10 min and then filtrated using a 0.22-μm cellulose nitrate membrane filter. An aliquot of the filtered solution was acidified with HNO<sub>3</sub> and was analyzed for the concentration of metal ions by inductively coupled plasma atomic emission spectrometry (ICP-AES, Agilent 720ES, USA). The amount of metal ions adsorbed by the biosorbent were calculated by following equation.

$$q_t = \frac{(C_0 - C_t)V}{W} \quad (1)$$

where  $q_t$  (mg/g) is the amount of adsorbed metal ions by the biosorbent at time  $t$  (h);  $C_0$  (mg/L) and  $C_t$  (mg/L) are the liquid phase concentration of metal ions at time 0 (h) and  $t$  (h), respectively;  $V$  (L) the volume of the solution, and  $W$  (g) the weight of the biosorbent.

To determine major parameters of adsorption kinetics, the pseudo-second-order rate equation [24] was used to elucidate the sorption process. The pseudo-second-order kinetic rate equation is:

$$\frac{t}{q_t} = \frac{1}{kq_e^2} + \frac{t}{q_e} \quad (2)$$

where  $q_e$  and  $q_t$  are the amounts of heavy metals adsorbed at time equilibrium and  $t$ , respectively;  $k$  is the rate constant of the pseudo-second-order adsorption.

### 2.5. Adsorption isotherms

Throughout the adsorption isotherm experiments, reaction conditions were controlled as follows: temperature 288.15–338.15 K, pH 6.0 ± 0.1, and metal ion 5–150 mg/L; volume of solution was 50 mL; the weight ratio of biosorbent to metal ions was 2.5/1. After 30 min of agitation in an isothermal shaker at 150 rpm for 30 min, samples were taken from the solutions and the metal concentration in the supernatants was measured with ICP-AES. The effect of temperature on the sorption capacity of metal ions onto the EPS was investigated. Langmuir, Freundlich, and Temkin adsorption models are used to describe the sorption phenomena of metal ions onto biosorbent.

The theoretical basis of the Langmuir equation relies on the assumption that intermolecular forces decrease rapidly with distance and consequently predicts the existence of monolayer coverage of the heavy metals at the outer surface of the adsorbent. The Langmuir isotherm equation is expressed as the linear function [25,26]:

$$\frac{1}{q_e} = \frac{1}{q_{\max}} + \left( \frac{1}{q_{\max} K_L} \right) \frac{1}{C_e} \quad (3)$$

where  $C_e$  is the equilibrium  $\text{Cu}^{2+}$  concentration in the solution (mg/L),  $q_{\max}$  is the monolayer sorption capacity of the biosorbent (mg/L), and  $K_L$  is the Langmuir constant (L/mg) and is related to the free energy of adsorption.

The sorption data were also fitted to the Freundlich isotherm, which assumes the exponential distribution of sorption sites and energies and the interaction between adsorbed molecules on the surface. The Freundlich equation is written as the logarithmic linear equation [24]:

$$\ln q_e = \ln K_F + \frac{1}{n} \ln C_e \quad (4)$$

where  $K_F$  (L/mg) $^{1/n}$  and  $n$  are Freundlich sorption isotherm constants being indicative of the extent of the adsorption and the degree of nonlinearity between solution concentration and adsorption, respectively.

Temkin isotherm assumes that decrease in the heat of adsorption is linear and the adsorption is characterized by a uniform distribution of binding energies [27]. The heat of sorption of all the molecules in the layer would decrease linearly with coverage due to sorbate/sorbent interactions [28]. Temkin isotherm is expressed by the following equation:

$$q_e = \frac{RT}{b_t} \ln(a_t C_e) \quad (5)$$

where  $a_t$  is equilibrium binding constant (L/mg),  $b_t$  is related to heat of adsorption (J/mol),  $R$  is the gas constant ( $8.314 \times 10^{-3}$  kJ/K mol), and  $T$  is the absolute temperature (K).

## 2.6. Adsorption thermodynamics

The thermodynamic parameters including Gibbs free energy change ( $\Delta G^\circ$ ), enthalpy change ( $\Delta H^\circ$ ), and entropy change ( $\Delta S^\circ$ ) are calculated according to the following thermodynamic equations [1]:

$$\Delta G^\circ = -RT \ln K_L \quad (6)$$

$$\Delta G^\circ = \Delta H^\circ - T\Delta S^\circ \quad (7)$$

where  $\Delta G^\circ$  is the change in free energy, kJ/mol;  $\Delta H^\circ$  is the change in enthalpy, kJ/mol;  $\Delta S^\circ$  is the change in entropy;  $K_L$  is from Langmuir equation constant,  $R$  is the gas constant (8.3144 J/mol K);  $T$  is the temperature in Kelvin, K. Equations can be obtained from Eqs. (7) and (8):

$$\ln K_L = \frac{\Delta S^\circ}{R} - \left( \frac{\Delta H^\circ}{R} \right) \frac{1}{T} \quad (8)$$

The application of Eq. (9) represents a mathematical relationship between  $K_L$  and  $1/T$ . The values of  $\ln K_L$  are plotted against those of  $1/T$ , and then  $\Delta H^\circ$  and  $\Delta S^\circ$  are calculated from the intercept and the slope of the plot, respectively. In addition, the values of  $\Delta G^\circ$  at various temperatures can be calculated according to Eq. (8).

## 2.7. Analytical methods

Protein, polysaccharide, and nucleic acid were examined as the major constituents of biosorbent using the following colorimetric methods [20]: Bradford method for protein content, bovine serum albumin as the standard; phenol-sulfuric acid method for polysaccharide content, glucose as the standard; diphenylamine colorimetric method for nucleic acid content, calf thymus deoxyribonucleic acid as the standard; Liquid chromatography (LC-10ADvp) with a gel filtration column (Tosoh TSK gel G4000PWXL,  $7.8 \times 300$  mm) was used to obtain the molecular weight of the biosorbent.

The analyses of scanning electron microscopy (SEM) image and energy dispersive X-ray (EDX) were completed using Philips XL 30 ESEM with a EDX spectroscopy at the electron accelerating voltage of 20.0 kV. The biosorbents before and after heavy metal adsorption were lyophilized and then for the analysis of functional groups with a Fourier transform infrared (FTIR) spectrometer Nicolet 5700 at room temperature, and the spectra were recorded in the wave number range of  $4,000\text{--}400$   $\text{cm}^{-1}$  at a resolution of  $5$   $\text{cm}^{-1}$  with 16 scans.

## 3. Results and discussion

### 3.1. Adsorption kinetics

To determine major parameters governing sorption kinetics, kinetic sorption data acquired empirically

were fitted to the Lagergren pseudo-second-order rate equation (Fig. 1), which has been widely used to describe metal and organic sorption onto different sorbents [29]. The results of regression are summarized in Table 1. With the initial concentration of metal ion increasing from 5 to 50 mg/L, the sorption capacity of  $\text{Pb}^{2+}$  and  $\text{Zn}^{2+}$  were increased from 59.62 to 416.67 mg/L and from 44.25 to 218.10 mg/L, respectively. The correlation coefficients ( $R^2$ ) for the linear plots using the pseudo-second-order model are above 0.9980 for all the investigated initial concentrations of both  $\text{Pb}^{2+}$  and  $\text{Zn}^{2+}$ . In addition, the  $q_e$  values of theoretical and experimental on both  $\text{Pb}^{2+}$  and  $\text{Zn}^{2+}$  show excellent agreement since the relative deviation is less than 5%, which is consistent with the previously reported for the sorption of heavy metals onto biosorbents [23,30].

### 3.2. Adsorption isotherms

The adsorption isotherms of  $\text{Pb}^{2+}$  and  $\text{Zn}^{2+}$  onto biosorbent are given in Fig. 2. Analysis of equilibrium data is important for developing an equation that can be used for design purposes. The effect of temperature on the sorption capacity of  $\text{Pb}^{2+}$  and  $\text{Zn}^{2+}$  onto the EPS was investigated. The adsorption constants estimated from the isotherms and the corresponding coefficients were given in Table 2. Langmuir models had a good agreement with the data for the adsorption of  $\text{Pb}^{2+}$  and  $\text{Zn}^{2+}$ , evidenced by the high  $R^2$  values (all greater than 0.980).

From simulation with Langmuir isotherm, raising the temperature from 298.15 to 328.15 K enabled increasing the sorption capacity of  $\text{Pb}^{2+}$  and  $\text{Zn}^{2+}$  onto the biosorbent from 451.20 to 793.61 mg/g and 267.07 to 408.38 mg/g, respectively. However, the sorption capacity of the biosorbent on the absorption of  $\text{Pb}^{2+}$  and  $\text{Zn}^{2+}$  showed a slight decrease simultaneously

when the temperature was further raised to 338.15 K, which might be due to the denaturing of biosorbent caused by the higher temperature [31]. The results also demonstrated that the sorption mechanism associated with the removal of  $\text{Pb}^{2+}$  and  $\text{Zn}^{2+}$  by the biosorbent involved a chemical sorption process.

From the corresponding Langmuir parameters, it was calculated the dimensionless parameter  $r$  or “separation factor”, which is defined as [6]:

$$K_R = \frac{1}{1 + K_L C_0} \quad (9)$$

According to the calculated  $K_R$  values,  $K_R = 0$  corresponds to irreversible adsorption,  $0 < K_R < 1$  to the favorable equilibrium,  $K_R = 1$  to the linear case, and  $K_R > 1$  to unfavorable equilibrium [6]. The values of  $K_R$  for sorption of  $\text{Pb}^{2+}$  and  $\text{Zn}^{2+}$  at 298.15, 308.15, 318.15, 328.15, and 338.15 K were given in Table 3. The values of  $K_R$  for sorption of  $\text{Pb}^{2+}$  and  $\text{Zn}^{2+}$  onto the biosorbent increased with the increasing initial concentration of  $\text{Pb}^{2+}$  and  $\text{Zn}^{2+}$ , respectively. All of the values were less than 1, indicating that the sorption process was favorable for all systems. The  $K_R$  values indicated that sorption was more favorable for the higher initial metal ion concentrations than for the lower ones.

### 3.3. Adsorption thermodynamics

The sorption thermodynamics were studied to gain an insight into the sorption behaviors. It can be seen from Fig. 3 that, the plot of  $\ln K_L$  for  $\text{Pb}^{2+}$  and  $\text{Zn}^{2+}$  vs.  $1/T$  was a straight line. The results of the thermodynamic calculations of  $\text{Pb}^{2+}$  and  $\text{Zn}^{2+}$  are shown in Table 4. The negative values for the Gibbs free energy of  $\text{Pb}^{2+}$  and  $\text{Zn}^{2+}$  show that the sorption process is

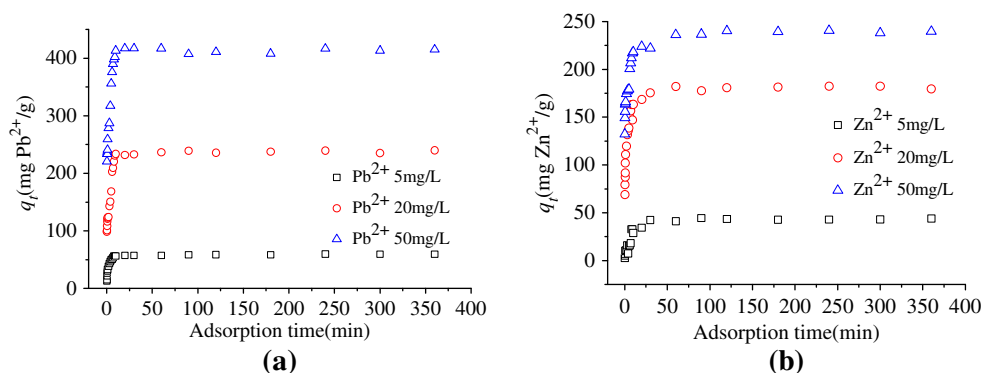


Fig. 1. Adsorption kinetics of  $\text{Pb}^{2+}$ : (a) and  $\text{Zn}^{2+}$  (b) onto the biosorbent.

Table 1

Pseudo-second-order equation parameters for three equilibrium  $\text{Pb}^{2+}$  and  $\text{Zn}^{2+}$  concentrations in the adsorption system of  $\text{Pb}^{2+}$  and  $\text{Zn}^{2+}$  onto the biosorbent

Metal ion	$C_0$ (mg/L)	$q_{e,\text{exp}}$ (mg/g)	$k_2$ (g/(mg min))	$q_{e,\text{cal}}$ (mg/g)	$R^2$
$\text{Pb}^{2+}$	5	59.69	0.0162	59.52	0.9999
	20	239.9	0.0059	238.1	0.9999
	50	417.35	0.0048	416.67	0.9999
$\text{Zn}^{2+}$	5	43.99	0.0043	44.25	0.9983
	20	182.42	0.0044	181.82	0.9999
	50	240.54	0.0041	238.10	1.0000

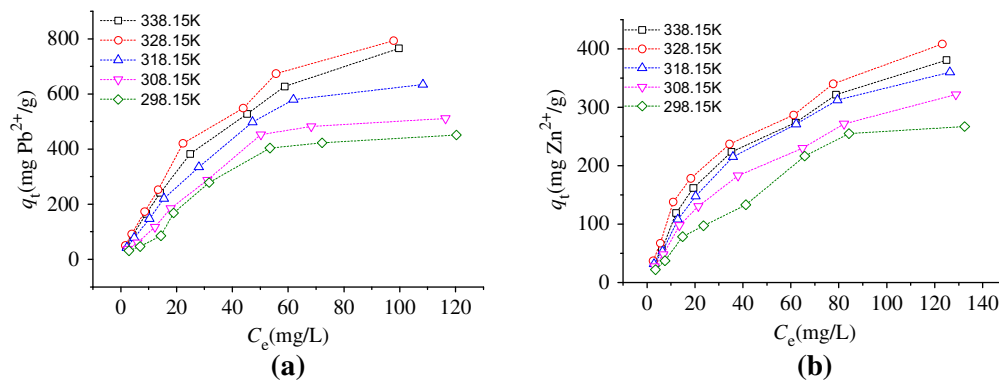


Fig. 2. Adsorption isotherms of  $\text{Pb}^{2+}$ : (a) and  $\text{Zn}^{2+}$  (b) onto the biosorbent.

Table 2

Langmuir, Freundlich, and Temkin model parameters under different temperature conditions in the adsorption system of  $\text{Pb}^{2+}$  and  $\text{Zn}^{2+}$  onto the biosorbent

Metal ion	Temperature (K)	$q_{\text{max,exp}}$ (mg/g)	Langmuir			Freundlich			Temkin		
			$q_{\text{max}}$ (mg/g)	$K_L$ (L/mg)	$R^2$	$k_f$ (L/mg) <sup>1/n</sup>	$n$	$R^2$	$a_t$	$b_t$	$R^2$
$\text{Pb}^{2+}$	338.15	765.29	769.23	0.034	0.9928	32.52	1.38	0.9898	0.3776	15.08	0.9197
	328.15	793.61	833.33	0.037	0.9886	38.39	1.41	0.9737	0.4336	14.09	0.9339
	318.15	634.39	666.67	0.031	0.9917	25.08	1.36	0.9784	0.3330	16.00	0.8956
	308.15	511.21	526.32	0.026	0.9871	16.44	1.21	0.9704	0.2814	17.80	0.8969
	298.15	451.20	454.55	0.024	0.9844	12.21	1.19	0.947	0.2383	18.54	0.8888
$\text{Zn}^{2+}$	338.15	380.76	416.66	0.030	0.9890	19.94	1.54	0.9694	0.3423	30.10	0.9667
	328.15	408.38	454.55	0.034	0.9957	26.02	1.65	0.9590	0.4167	28.72	0.9721
	318.15	360.01	384.62	0.030	0.9862	17.47	1.51	0.9784	0.3122	28.99	0.9562
	308.15	321.95	344.83	0.027	0.9923	14.61	1.50	0.9795	0.2875	31.89	0.9428
	298.15	267.07	285.71	0.023	0.9874	9.51	1.40	0.9798	0.2255	33.80	0.8856

feasible and spontaneous in nature and that the degree of spontaneity of the reaction for both  $\text{Pb}^{2+}$  and  $\text{Zn}^{2+}$  increases with increasing temperature. The results of adsorption isotherms also demonstrate that adsorption capacity of  $\text{Pb}^{2+}$  and  $\text{Zn}^{2+}$  increase with increasing temperature. The overall sorption process of  $\text{Pb}^{2+}$  and  $\text{Zn}^{2+}$  onto the biosorbent seem to be

endothermic nature which can be confirmed by the positive values of  $\Delta H^\circ$  of both  $\text{Pb}^{2+}$  (11.50 kJ/mol) and  $\text{Zn}^{2+}$  (10.58 kJ/mol). The  $\Delta G^\circ$  value is in the range of 0–20 kJ/mol and –80 to –400 kJ/mol for physical and chemical adsorptions, respectively [32]. In this study, the  $\Delta G^\circ$  values are in the range of –21.02 to –24.35 kJ/mol, indicating that the adsorptions are

Table 3  
 $K_R$  values based on the Langmuir isotherm

$C_0$ (mg/L)	298.15 K		308.15 K		318.15 K		328.15 K		338.15 K	
	Pb <sup>2+</sup>	Zn <sup>2+</sup>								
5	0.893	0.897	0.885	0.881	0.866	0.870	0.8439	0.8547	0.8547	0.8696
10	0.806	0.813	0.794	0.787	0.763	0.769	0.7299	0.7463	0.7463	0.7692
20	0.676	0.685	0.658	0.649	0.617	0.625	0.5747	0.5952	0.5952	0.6250
30	0.581	0.592	0.562	0.552	0.518	0.526	0.4739	0.4950	0.4950	0.5263
40	0.510	0.521	0.49	0.481	0.446	0.455	0.4032	0.4237	0.4237	0.4545
50	0.455	0.465	0.435	0.426	0.392	0.400	0.3509	0.3704	0.3704	0.4000
80	0.342	0.352	0.325	0.316	0.287	0.294	0.2525	0.2688	0.2688	0.2941
100	0.294	0.303	0.278	0.270	0.244	0.250	0.2128	0.2273	0.2273	0.2500

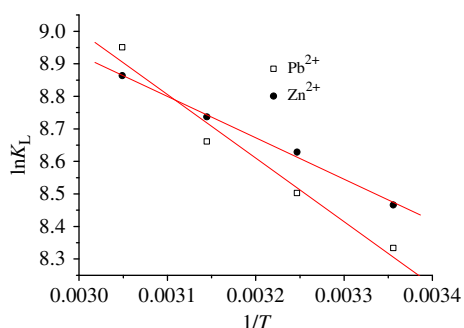


Fig. 3. Plots of the kinetic constant ( $\ln K_L$ ) vs. temperature ( $1/T$ ) for the biosorbent adsorbing Pb<sup>2+</sup> and Zn<sup>2+</sup>.

mainly physisorption in nature enhanced by chemisorption. The positive value of  $\Delta S^\circ$  suggests an increased randomness at the solid/solution interface with some structural changes in the adsorbate and the adsorbent, and an affinity of the adsorbent [33].

#### 3.4. Adsorption mechanisms

The SEM micrographs of heavy metal-free and metal-loaded biosorbents are shown in Fig. 4. The biosorbent showed a meshy structure with small branches. During the sorption process, the biosorbent reacted with the metal ions in the solutions, and

became precipitates to be separate from the solutions. After adsorption of Pb<sup>2+</sup> and Zn<sup>2+</sup>, the precipitates like a well-knit net were separate from water, which revealed the excellent adsorption performance of the biosorbent. The precipitate of the Pb<sup>2+</sup> adsorption by the biosorbent was found to be compact, which was different from that of the Zn<sup>2+</sup> adsorption.

The EDX analyses were conducted to understand the element variations of heavy metal-free and metal-loaded biosorbents. Fig. 5 showed the EDX spectra of the samples. The major elements found in the biosorbent were composed of C, N, O, K, Na, and Mg. After Pb<sup>2+</sup> and Zn<sup>2+</sup> adsorption, the EDX spectra of the precipitates clearly showed the presence of the adsorbed metal elements. Moreover, other elements in the precipitates were consistent with those in the biosorbent. Accordingly, the removal of the metal ions was achieved via the adsorption of the biosorbent.

The FTIR spectra of the biosorbent before and after Pb<sup>2+</sup> and Zn<sup>2+</sup> adsorption are shown in Fig. 6, and the main sharp stretching frequencies from the spectra and the biological molecule involved are proposed in Table 5 according to the literature data. All of the heavy metal-free and metal-loaded biosorbent samples display a broad stretching intense peak at around 3,400 cm<sup>-1</sup> characteristic for –OH (mainly existing in phenolic, alcoholic hydroxyl and polysaccharide) and –NH<sub>2</sub> [19,20,34,35]. It can be noticed that new adsorption band

Table 4  
 Thermodynamic parameters calculated for the sorption of Pb<sup>2+</sup> and Zn<sup>2+</sup> onto the biosorbent

Metal ion	$\Delta G^\circ$ (kJ/mol)				$\Delta H^\circ$ (kJ/mol)	$\Delta S^\circ$ (J/mol K)	$R^2$
	298 K	308 K	318 K	328 K			
Pb <sup>2+</sup>	-21.07	-22.16	-23.25	-24.35	11.50	109.24	0.9741
Zn <sup>2+</sup>	-21.02	-22.08	-23.14	-24.20	10.58	106.00	0.9959

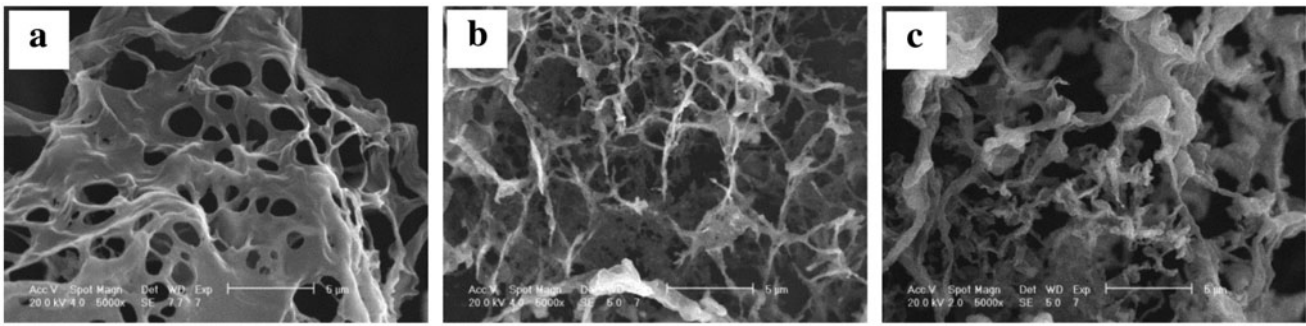


Fig. 4. SEM images of the biosorbent: (a) before and after (b)  $Pb^{2+}$  and (c)  $Zn^{2+}$  adsorption.

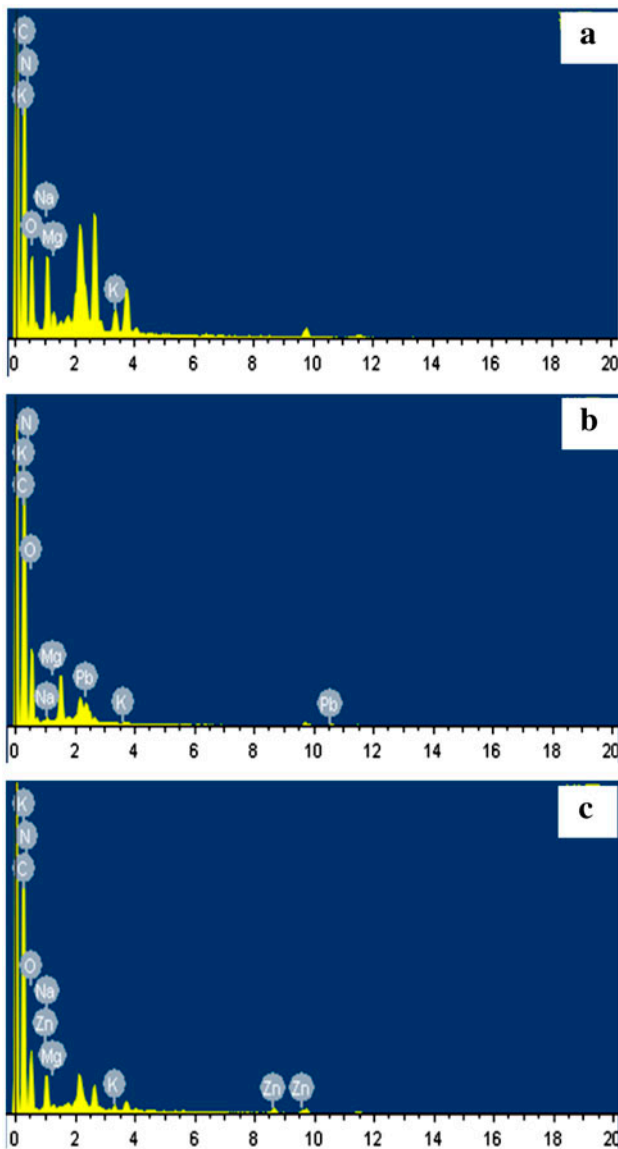


Fig. 5. EDX images of the biosorbent: (a) before and after (b)  $Pb^{2+}$  and (c)  $Zn^{2+}$  adsorption.

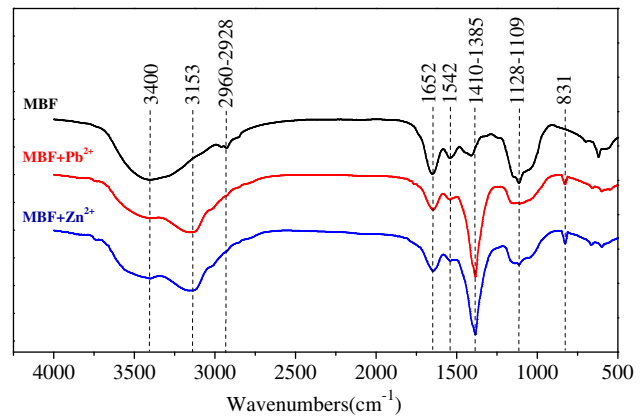


Fig. 6. FTIR spectra of the biosorbent before and after adsorbing  $Pb^{2+}$  and  $Zn^{2+}$ .

at around  $3,153\text{ cm}^{-1}$  appeared after the biosorbent adsorbing  $Zn^{2+}$  and  $Pb^{2+}$ . The disappearance of peaks between  $2,960$  and  $2,928\text{ cm}^{-1}$  for the biosorbent adsorbing  $Pb^{2+}$  and  $Zn^{2+}$  indicates that  $-CH_2-$  asymmetric stretching vibration as a consequence of the adsorption [19,23,35,36]. Since  $-OH$ ,  $-NH_2$ , and  $-CH_2-$  cannot dissociate hydrogen ions at the pH 6.0, the complexation between the functional groups and the metal ions should take place during the sorption process [37,38]. The absorption bands at around  $1,652\text{ cm}^{-1}$  are characteristic for stretching vibration of  $-COOH$  stretching vibration, the obvious shift in  $-COOH$  and  $C-N$  (Amide I) after the adsorption of  $Pb^{2+}$  and  $Zn^{2+}$  indicates that hydrogen ions exist in carboxyl groups were replaced by  $Pb^{2+}$  and  $Zn^{2+}$ . Thus, ion exchange between the functional groups and the metal ions should also take place during the sorption process [19,20,23,36]. The adsorption band at  $1,542\text{ cm}^{-1}$  characteristic is for stretching vibration of  $C-N$  and deformation vibration of  $N-H$  of Amide II in proteins, and their decline after the adsorption means they participated in the sorption process [19,20,23,38]. The adsorption band of three samples

Table 5  
Main functional groups observed from FTIR spectra of the biosorbent

No.	Wave number (cm <sup>-1</sup> )	Vibration type	References
1	3,400	Stretching vibration of OH and NH	[10,11,28,29]
2	3,153	Stretching vibration of OH and vibration of NH	[30,31]
3	2,960–2,928	Asymmetric stretching vibration of CH <sub>2</sub>	[4,10,29,32]
4	1,652	Stretching vibration of COOH and CN (Amide I)	[10,11,14,32]
5	1,542	Stretching vibration of CN and deformation vibration of NH (Amide II)	[10,11,14,31]
6	1,410–1,385	Stretching vibration of C=O Deformation vibration of OH	[14,31,32]
7	1,128–1,109	Stretching vibration C–O–C and C=C	[10,14,32]
8	831	“Fingerprint” zone Several bands visible	[13,30]

between 1,410 and 1,385 cm<sup>-1</sup> is characteristic for stretching vibration of C=O and deformation vibration of –OH, which were contained in carboxylates and phenolic hydroxyl, respectively [23,36,38]. The structure of the groups changed after the adsorption of Pb<sup>2+</sup> and Zn<sup>2+</sup> due to the obvious shift. The adsorption peak between 1,128 and 1,109 cm<sup>-1</sup> indicates the stretching vibration of C=C and asymmetric stretching vibration of C–O–C which were involved in the sorption process because of the palpable deviation [19,23,36]. Apparently, new peak was formed at 831 cm<sup>-1</sup> which also called “Fingerprint” zone characteristic for phosphate or sulfur functional groups [22,37].

Adsorption kinetic, isotherm, thermodynamic, and SEM analyses indicated that the adsorption of the biosorbent for Pb<sup>2+</sup> and Zn<sup>2+</sup> was mainly physisorption in nature enhanced by chemisorption. EDX and FTIR spectra analyses further revealed that complexation and ion exchange between the functional groups and the metal ions played an important role in the chemisorption.

#### 4. Concluding remarks

The present study discloses the adsorption characterizations of the biosorbent extracted from WAS after short-time aerobic digestion for Pb<sup>2+</sup> and Zn<sup>2+</sup>. The adsorption kinetics were well fit for the pseudo-second-order model. The adsorption isotherms could be described by the Langmuir model. The Gibbs free energy analyses showed that the sorption processes were feasible and spontaneous in nature. The surface morphology of the heavy metal-free biosorbent showed a meshy structure with small branches. The EDX spectra of the precipitates confirmed that the metal elements were settled by the biosorbent. FTIR analyses showed that the major functional groups are responsible for the adsorption. The adsorption of the biosorbent for Pb<sup>2+</sup> and Zn<sup>2+</sup> was mainly physisorption

in nature enhanced by chemisorption. Complexation and ion exchange between the functional groups and the metal ions played an important role in the chemisorption.

#### Acknowledgements

The authors sincerely acknowledge the support provided by China Scholarship Council, the National Science & Technology Pillar Program (2013BAD21B03), and the higher school innovative engineering plan (111 Project).

#### Abbreviations

WAS	—	waste activated sludge
EPS	—	extracellular polymeric substances
WWTP	—	wastewater treatment plant
VSS	—	volatile suspended solids
SS	—	suspended solids
DO	—	dissolved oxygen
SEM	—	scanning electron microscopy
EDX	—	energy dispersive X-Ray spectroscopy
FTIR	—	fourier transform infrared

#### References

- [1] A.Y. Dursun, A comparative study on determination of the equilibrium, kinetic and thermodynamic parameters of biosorption of copper(II) and lead(II) ions onto pretreated *Aspergillus niger*, *Biochem. Eng. J.* 28 (2006) 187–195.
- [2] M.A. Ashraf, M. Ahmad, S. Akib, K.S. Balkhair, N.K. Abu Bakar, Chemical species of metallic elements in the aquatic environment of an ex-mining catchment, *Water Environ. Res.* 86 (2014) 717–728.
- [3] M.A. Ashraf, I. Yusoff, M. Yusof, Y. Alias, Study of contaminant transport at an open-tipping waste disposal site, *Environ. Sci. Pollut. Res. Int.* 20 (2013) 4689–4710.

- [4] P. Chave, The EU Water Framework Directive: An Introduction, IWA publishing, London, 2001.
- [5] R. Naseem, S.S. Tahir, Removal of Pb(II) from aqueous/acidic solutions by using bentonite as an adsorbent, *Water Res.* 35 (2001) 3982–3986.
- [6] F. Rozada, M. Otero, A. Moran, A.I. Garcia, Adsorption of heavy metals onto sewage sludge-derived materials, *Bioresour. Technol.* 99 (2008) 6332–6338.
- [7] D.W. O'Connell, C. Birkinshaw, T.F. O'Dwyer, Heavy metal adsorbents prepared from the modification of cellulose: A review, *Bioresour. Technol.* 99 (2008) 6709–6724.
- [8] H.H. Nur, Y. Ismail, A. Yatimah, M. Sharifah, Y.R. Nurul, A.A. Muhammad, Ionic liquid as a medium to remove iron and other metal ions: A case study of the North Kelantan Aquifer, Malaysia, *Environ. Earth Sci.* 71 (2014) 2105–2113.
- [9] J.F. Blais, S. Dufresne, G. Mercier, State of the art of technologies for metal removal from industrial effluents, *Rev. Sci. Eau* 12 (1999) 687–711.
- [10] S. Batool, S. Akib, M. Ahmad, K.S. Balkhair, M.A. Ashraf, Study of modern nano enhanced techniques for removal of dyes and metals, *J. Nanomater.* 2014 (2014) 1–20.
- [11] Z.Q. Zhang, P. Wang, J. Zhang, S.Q. Xia, Removal and mechanism of Cu(II) and Cd(II) from aqueous single-metal solutions by a novel biosorbent from waste activated sludge, *Environ. Sci. Pollut. Res.* 21 (2014) 10823–10829.
- [12] B.Y. Chen, V.P. Utgikar, S.M. Harmon, H.H. Tabak, D.F. Bishop, R. Govind, Studies on biosorption of zinc (II) and copper(II) on *Desulfovibrio desulfuricans*, *Int. Biodeterior. Biodegrad.* 46 (2000) 11–18.
- [13] T. Schwartz, S. Hoffmann, U. Obst, Formation and bacterial composition of young, natural biofilms obtained from public bank-filtered drinking water systems, *Water Res.* 32 (1998) 2787–2797.
- [14] X.Y. Li, B.E. Logan, Collision frequencies of fractal aggregates with small particles by differential sedimentation, *Environ. Sci. Technol.* 31 (1997) 1229–1236.
- [15] A.A. Muhammad, H. Masroor, M. Karamat, W. Abdul, Y. Mohamad, A. Yatimah, Y. Ismail, Removal of acid yellow-17 dye from aqueous solution using ecofriendly biosorbent, *Desalin. Water Treat.* 51(22–24) (2013) 4530–4545.
- [16] A.A. Muhammad, A.R. Muhammad, A. Yatimah, Y. Ismail, Removal of Cd(II) onto *Raphanus sativus* peels biomass: Equilibrium, kinetics, and thermodynamics, *Desalin. Water Treat.* 51(22–24) (2013) 4402–4412.
- [17] Z.Q. Zhang, S.Q. Xia, X.J. Wang, A.M. Yang, B. Xu, L. Chen, Z.L. Zhang, J. Zhao, N. Jaffrezic-Renault, D. Leonard, A novel biosorbent for dye removal: Extracellular polymeric substance (EPS) of *Proteus mirabilis* TJ-1, *J. Hazard. Mater.* 163 (2009) 279–284.
- [18] T.T. More, S. Yan, N.V. Hoang, R.D. Tyagi, R.Y. Surampalli, Bacterial polymer production using pretreated sludge as raw material and its flocculation and dewatering potential, *Bioresour. Technol.* 121 (2012) 425–431.
- [19] G. Guibaud, S. Comte, F. Bordas, S. Dupuy, M. Baudu, Comparison of the complexation potential of extracellular polymeric substances (EPS), extracted from activated sludges and produced by pure bacteria strains, for cadmium, lead and nickel, *Chemosphere* 59 (2005) 629–638.
- [20] G. Guibaud, N. Tixier, A. Bouju, M. Baudu, Relation between extracellular polymers' composition and its ability to complex Cd, Cu and Pb, *Chemosphere* 52 (2003) 1701–1710.
- [21] Y. Liu, H.H.P. Fang, Influences of extracellular polymeric substances (EPS) on flocculation, settling, and dewatering of activated sludge, *Crit. Rev. Environ. Sci. Technol.* 33 (2003) 237–273.
- [22] J.J. Zhong, T. Yoshida, High-density cultivation of *Perilla frutescens* cell suspensions for anthocyanin production: Effects of sucrose concentration and inoculum size, *Enzyme Microb. Technol.* 17 (1995) 1073–1079.
- [23] G. Guibaud, S. Comte, F. Bordas, M. Baudu, Metal removal from single and multimetallic equimolar systems by extracellular polymers extracted from activated sludges as evaluated by SMDE polarography, *Process Biochem.* 40 (2005) 661–668.
- [24] S. Comte, G. Guibaud, M. Baudu, Biosorption properties of extracellular polymeric substances (EPS) towards Cd, Cu and Pb for different pH values, *J. Hazard. Mater.* 151 (2008) 185–193.
- [25] J.S. Kwon, S.T. Yun, J.H. Lee, S.O. Kim, H.Y. Jo, Removal of divalent heavy metals (Cd, Cu, Pb, and Zn) and arsenic(III) from aqueous solutions using scoria: Kinetics and equilibria of sorption, *J. Hazard. Mater.* 174 (2010) 307–313.
- [26] T. Noshabah, R. Uzaira, S.B. Khaled, A.A. Muhammad, Chemodynamics of methyl parathion and ethyl parathion: Adsorption models for sustainable agriculture, *Biomed. Res. Int.* 2014 (2014) 831989.
- [27] W.T. Tsai, C.W. Lai, K.J. Hsien, Adsorption kinetics of herbicide paraquat from aqueous solution onto activated bleaching earth, *Chemosphere* 55 (2004) 829–837.
- [28] A. Günay, E. Arslankaya, İ. Tosun, Lead removal from aqueous solution by natural and pretreated clinoptilolite: Adsorption equilibrium and kinetics, *J. Hazard. Mater.* 146 (2007) 362–371.
- [29] M. Hosseini, S.F.L. Mertens, M. Ghorbani, M.R. Arshadi, Asymmetrical Schiff bases as inhibitors of mild steel corrosion in sulphuric acid media, *Mater. Chem. Phys.* 78 (2003) 800–808.
- [30] W.B. Lu, J.J. Shi, C.H. Wang, J.S. Chang, Biosorption of lead, copper and cadmium by an indigenous isolate *Enterobacter* sp. J1 possessing high heavy-metal resistance, *J. Hazard. Mater.* 134 (2006) 80–86.
- [31] B.J. Ni, R.J. Zeng, F. Fang, J. Xu, G.P. Sheng, H.Q. Yu, A novel approach to evaluate the production kinetics of extracellular polymeric substances (EPS) by activated sludge using weighted nonlinear least-squares analysis, *Environ. Sci. Technol.* 43 (2009) 3743–3750.
- [32] K.O. Adebawale, I.E. Unuabonah, B.I. Olu-Owolabi, The effect of some operating variables on the adsorption of lead and cadmium ions on kaolinite clay, *J. Hazard. Mater.* 134 (2006) 130–139.
- [33] Z.Q. Zhang, Y. Zhou, J. Zhang, S.Q. Xia, Copper (II) adsorption by the extracellular polymeric substance extracted from waste activated sludge after short-time aerobic digestion, *Environ. Sci. Pollut. Res.* 21 (2014) 2132–2140.

- [34] G.P. Sheng, J. Xu, H.W. Luo, W.W. Li, W.H. Li, H.Q. Yu, Z. Xie, S.Q. Wei, F.C. Hu, Thermodynamic analysis on the binding of heavy metals onto extracellular polymeric substances (EPS) of activated sludge, *Water Res.* 47 (2013) 607–614.
- [35] M. Iqbal, A. Saeed, S.I. Zafar, FTIR spectrophotometry, kinetics and adsorption isotherms modeling, ion exchange, and EDX analysis for understanding the mechanism of  $\text{Cd}^{2+}$  and  $\text{Pb}^{2+}$  removal by mango peel waste, *J. Hazard. Mater.* 164 (2009) 161–171.
- [36] Purwoko, H.G. Adang, D.C.N.A. Maskur, Preparasi  $^{131}\text{I}$ -mibg: Radiofarmaka diagnosa and terapi neuroblastoma (Preparation of  $^{131}\text{I}$ -mibg: Radiopharmaceutical for diagnosis and therapy neuroblastoma), Seminar Nasional VI Sdm Teknologi Nuklir VI, Yogyakarta 18 (2010) 695–704.
- [37] M. Jackson, H.H. Mantsch, The use and misuse of FTIR spectroscopy in the determination of protein structure, *Crit. Rev. Biochem. Mol. Biol.* 30 (1995) 95–120.
- [38] A.P. Terzyk, The influence of activated carbon surface chemical composition on the adsorption of acetaminophen (paracetamol) in vitro, *Colloids Surf., A.* 177 (2001) 23–45.